Available online at www.sciencedirect.com
SCIENCE DIRECT®
Catalysis Today 87 (2003) 219–226
CATALYSIS TODAY
www.elsevier.com/locate/cattod

# Preparation of new solid superacid catalyst, zirconium sulfate supported on γ-alumina and activity for acid catalysis

Jong Rack Sohn*, Dong Hee Seo

*Department of Industrial Chemistry, Engineering College, Kyungpook National University, Taegu 702-701, South Korea*

**Abstract**

Zirconium sulfate supported on γ-$Al_2O_3$ catalysts were prepared by impregnation of powdered γ-$Al_2O_3$ with zirconium sulfate aqueous solution followed by calcining in air at high temperature. For $Zr(SO_4)_2$/γ-$Al_2O_3$ samples, no diffraction line of zirconium sulfate was observed up to 50 wt.%, indicating good dispersion of $Zr(SO_4)_2$ on the surface of γ-$Al_2O_3$. The acidity of catalysts increased in proportion to the zirconium sulfate content up to 40 wt.% of $Zr(SO_4)_2$. 40-$Zr(SO_4)_2$/γ-$Al_2O_3$ calcined at 400 °C exhibited maximum catalytic activities for 2-propanol dehydration and cumene dealkylation. The catalytic activities for both reactions, 2-propanol dehydration and cumene dealkylation were correlated with the acidity of catalysts measured by ammonia chemisorption method.
© 2003 Elsevier B.V. All rights reserved.

*Keywords:* Zirconium sulfate; Characterization; 2-Propanol dehydration; Cumene dealkylation; Acidic properties

## 1. Introduction

Acid catalysis is of fundamental industrial importance. Solid acid catalysts play an important role in hydrocarbon conversion reactions in the chemical and petroleum industries, and environmentally benign chemical processes [1,2]. Many kinds of solid acids have been found. Their acidic properties on catalyst surfaces, their catalytic action, and the structure of acid sites have been elucidated for a long time, and those results have been reviewed by Arata [3]. The potential for a heterogeneous catalyst has yielded many papers on the catalytic activity of sulfated zirconia materials [3–7]. Sulfated zirconia incorporating Fe and Mn has been shown to be highly active for butane isomerization, catalyzing the reaction even at room temperature [8,9].

It has been reported by several workers that the addition of platinum to zirconia modified by sulfate ions enhances catalytic activity in the skeletal isomerization of alkanes without deactivation when the reaction is carried out in the presence of hydrogen [10–12]. The high catalytic activity and small deactivation can be explained by both the elimination of the coke by hydrogenation and hydrogenolysis [10], and the formation of Brönsted acid sites from $H_2$ on the catalysts [11].

On the other hand, many metal sulfates generate fairly large amounts of acid sites of moderate or strong strength on their surfaces when they are calcined at 400–700 °C [2,13]. The acidic property of metal sulfate often gives high selectivity for diversified reactions such as hydration, polymerization, alkylation, cracking, and isomerization [2,13]. However, structural and physicochemical properties of supported metal sulfates are considered to be in different states compared with bulk metal sulfates because of their interaction with supports [14]. Zirconium sulfate

* Corresponding author. Tel.: +82-53-950-5585; fax: +82-53-950-6594.
*E-mail address:* jrsohn@knu.ac.kr (J.R. Sohn).

0920-5861/$ – see front matter © 2003 Elsevier B.V. All rights reserved.
doi:10.1016/j.cattod.2003.09.010

catalysts supported on γ-$Al_2O_3$ have not been reported up to now.

This paper describes the characterization of zirconium sulfate supported on γ-alumina and its acid catalytic properties for the volatile organic chemicals. The characterization of the samples was performed by means of Fourier transform infrared (FTIR), X-ray diffraction (XRD), differential scanning calorimetry (DSC), and surface area measurements. For the acid catalysis for the volatile organic chemicals, the 2-propanol dehydration and cumene dealkylation were used as test reactions.

## 2. Experimental

The catalysts containing various zirconium sulfate (Junsei Chemical Co.) contents were prepared by adding an aqueous solution of zirconium sulfate [$Zr(SO_4)_2 \cdot 4H_2O$] to the γ-$Al_2O_3$ powder (JRC-ALO-2, surface area = 240 $m^2/g$) followed by drying and calcining at high temperatures for 2 h in air. This series of catalysts are denoted by their weight percentage of $Zr(SO_4)_2$. For example, 10-$Zr(SO_4)_2$/γ-$Al_2O_3$ indicates the catalyst containing 10 wt.% $Zr(SO_4)_2$.

FTIR spectra were obtained in a heatable gas cell at room temperature using Mattson Model GL6030E FTIR spectrophotometer. The self-supporting catalyst wafers contained about 9 $mg/cm^2$. Prior to obtaining the spectra, the sample were heated under vacuum at 400–500 °C for 1.5 h.

Catalysts were checked in order to determine the structure of the catalysts by means of a Philips X'pert-APD X-ray diffractometer, employing Cu Kα (Ni-filtered) radiation.

DSC measurements were performed in air by a PL-STA model 1500H apparatus, and the heating rate was 5 °C/min. For each experiment, 10–15 mg of sample was used.

The specific surface area was determined by applying the BET method to the adsorption of $N_2$ at −196 °C. Chemisorption of ammonia was also employed as a measure of the acidity of catalysts. The amount of chemisorption was determined based on the irreversible adsorption of ammonia [15–17].

2-Propanol dehydration was carried out at 160–180 °C in a pulse micro-reactor connected to a gas chromatograph. Fresh catalyst in the reactor made of 0.64 cm stainless steel was pretreated at 400 °C for 1 h in the nitrogen atmosphere. Diethyleneglycol succinate on Shimalite was used as packing material of gas chromatograph and the column temperature was 150 °C for analyzing the product. Catalytic activity for 2-propanol dehydration was represented as mole of propylene converted from 2-propanol per gram of catalyst. Cumene dealkylation was carried out at 400–450 °C in the same reactor as above. Packing material for the gas chromatograph was Benton 34 on chromosorb W and column temperature was 130 °C. Catalytic activity for cumene dealkylation was represented as mole of benzene converted from cumene per gram of catalyst. Conversion for both reactions were taken as the average of the first to sixth pulse values.

## 3. Results and discussion

### 3.1. Infrared spectra

The IR spectra of 20-$Zr(SO_4)_2$/γ-$Al_2O_3$ (KBr disc) calcined at different temperatures (400–900 °C) are given in Fig. 1. 20-$Zr(SO_4)_2$/γ-$Al_2O_3$ calcined up to 700 °C showed IR absorption bands at 1211, 1130, 1060 and 997 $cm^{-1}$ which are assigned to bidentate sulfate ion coordinated to the metal such as $Zr^{4+}$ or $Al^{3+}$ [17]. However, for the calcination of 800–900 °C IR bands by the sulfate ion disappeared due to the complete decomposition of sulfate ion, as shown in Fig. 1.

In general, for the metal oxides modified with sulfate ion followed by evacuating above 400 °C, a strong band assigned to S=O stretching frequency is observed at 1380–1370 $cm^{-1}$ [18–20]. In this work, the corresponding band for samples exposed to air was not found because water molecules in air were adsorbed on the surfaces of catalysts. These results are very similar to those reported by other authors [18–20]. However, in a separate experiment, IR spectra of self-supported 20-$Zr(SO_4)_2$/γ-$Al_2O_3$ after evacuation at 100–500 °C for 2 h were examined. As shown in Fig. 2, there were the intense band at 1380–1394 $cm^{-1}$ accompanied by broad and intense bands below 1250 $cm^{-1}$ due to the overlapping of the γ-$Al_2O_3$ skeletal vibration, indicating the presence of different adsorbed species

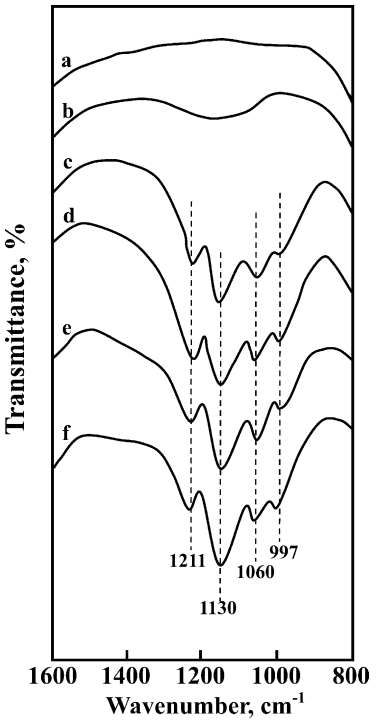


Fig. 1. Infrared spectra of 20-$Zr(SO_4)_2/\gamma$-$Al_2O_3$ calcined at different temperatures for 2 h: (a) 900 °C; (b) 800 °C; (c) 700 °C; (d) 600 °C; (e) 500 °C; (f) 400 °C.

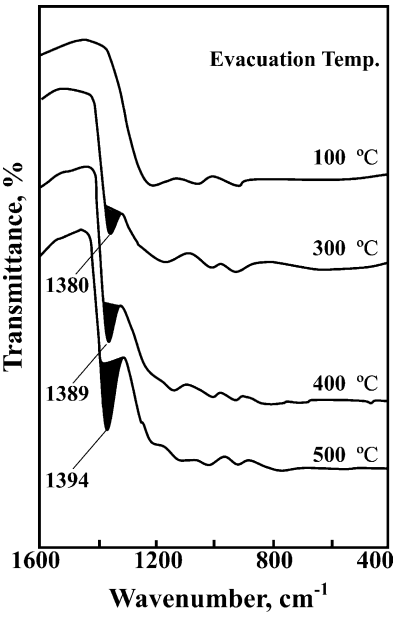


Fig. 2. Infrared spectra of 20-$Zr(SO_4)_2/\gamma$-$Al_2O_3$ evacuated at different temperatures.

depending on the treatment conditions of the sulfated sample [19]. At 100 °C, an asymmetric stretching band of S=O bonds was not observed because the water molecules are adsorbed on the surface of 20-$Zr(SO_4)_2/\gamma$-$Al_2O_3$ [20–22]. The band intensity increased with the evacuation temperature and the position of band shifted to a higher wavenumber. That is, the higher the evacuation temperature, the larger the shift of the asymmetric stretching frequency of the S=O bonds. It is likely that the surface sulfur complexes formed by the interaction of oxides with sulfate ions in highly active catalysts have a strong tendency to reduce their bond order by the adsorption of basic molecules such as $H_2O$ [20–22]. This frequency shift corresponding to a decrease in the bond order of SO covalent double bond and an increase in the partial charge on oxygen atom is associated with the acid strength of the catalyst [20–22]. The electron structures of the sulfur complex before and after water adsorption may be illustrated as follows:

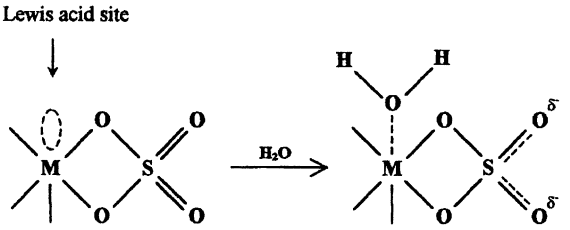


Consequently, as shown in Fig. 2, an asymmetric stretching band of S=O bonds for the sample evacuated at lower temperature appears at a lower frequency compared with that for the sample evacuated at higher temperature because of the adsorbed water.

### 3.2. *Crystalline structure of $Zr(SO_4)_2/\gamma$-$Al_2O_3$*

The crystalline structure of 40-$Zr(SO_4)_2/\gamma$-$Al_2O_3$ calcined in air at different temperatures for 2 h were checked by X-ray diffraction. For the 40-$Zr(SO_4)_2/\gamma$-$Al_2O_3$, as shown in Fig. 3, X-ray diffraction data indicated only $\gamma$-$Al_2O_3$ phase at 400–700 °C. However, at 800 °C, a tetragonal phase of $ZrO_2$ was observed due to the decomposition of zirconium sulfate, showing

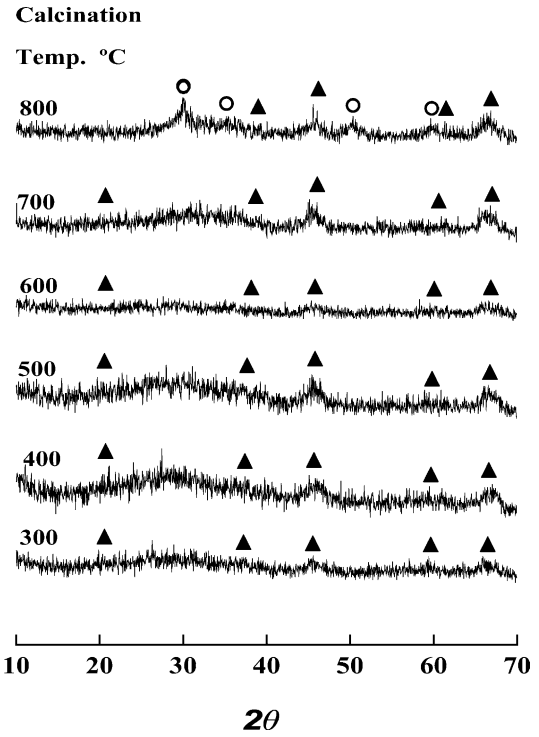


Fig. 3. X-ray diffraction patterns of 40-$Zr(SO_4)_2/\gamma$-$Al_2O_3$ calcined at different temperatures for 2 h: (○) tetragonal phase of $ZrO_2$; (▲) $\gamma$-$Al_2O_3$.

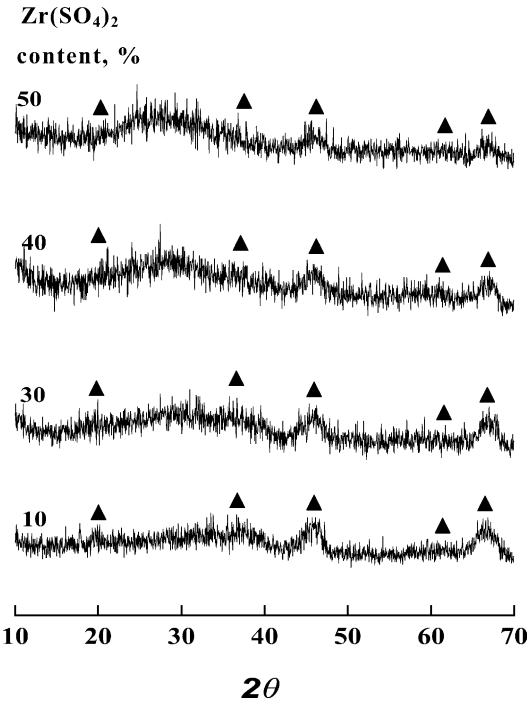


Fig. 4. X-ray diffraction patterns of $Zr(SO_4)_2/\gamma$-$Al_2O_3$ having various $Zr(SO_4)_2$ contents and calcined at 400 °C for 2 h: (▲) $\gamma$-$Al_2O_3$.

good agreement with the results of infrared spectra analysis mentioned above.

The XRD patterns of $Zr(SO_4)_2/\gamma$-$Al_2O_3$ containing different zirconium sulfate contents and calcined at 400 °C for 2 h are shown in Fig. 4. No diffraction line of zirconium sulfate is observed up to 50 wt.%, indicating good dispersion of $Zr(SO_4)_2$ on the surface of $\gamma$-$Al_2O_3$ due to the interaction between them.

### 3.3. Thermal analysis

To examine the thermal properties of precursors of $Zr(SO_4)_2/\gamma$-$Al_2O_3$ samples more clearly, thermal analysis has been carried out and the results are illustrated in Fig. 5. For pure $Zr(SO_4)_2{\cdot}4H_2O$, the DSC curve shows four endothermic peaks below 400 °C, due to water elimination, indicating that the dehydration of $Zr(SO_4)_2{\cdot}4H_2O$ occurs in four steps. The endothermic peak around 724 °C is due to the evolution of $SO_3$ decomposed from zirconium sulfate [23]. Zirconium sulfate begins to decompose around 700 °C, as shown in Fig. 4. Sohn and Park reported that sulfate ion bonded to zirconia decomposes around 700 °C [22].

However, for $Zr(SO_4)_2/\gamma$-$Al_2O_3$ samples, the DSC patterns are somewhat different from that of $Zr(SO_4)_2{\cdot}4H_2O$. For $Zr(SO_4)_2/\gamma$-$Al_2O_3$ samples, the DSC curve showed broad endothermic peaks below 200 °C due to the elimination of adsorbed water and the endothermic peaks around 830 °C due to the evolution of $SO_3$ decomposed from the sulfate ion bonded to the surface of $\gamma$-$Al_2O_3$ [23]. Namely, the thermal stability of the sulfate ion bonded to the surface of $\gamma$-$Al_2O_3$ is higher than that of zirconium sulfate by about 100 °C. In the case of $NiSO_4/\gamma$-$Al_2O_3$ samples reported previously, two endothermic peaks are observed around 785 and 829 °C due to the evolution of $SO_3$, showing that sulfated species with different thermal stability values are present in the samples [22].

### 3.4. Surface properties

It is necessary to examine the effect of zirconium sulfate on the surface properties of catalysts; that is,

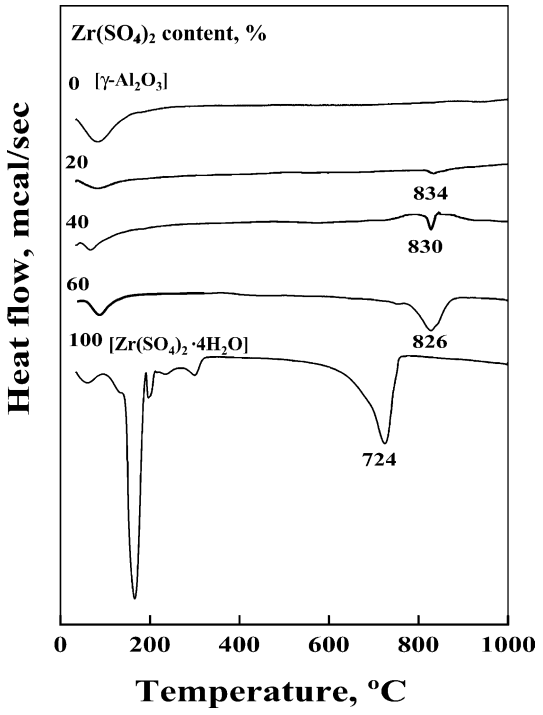


Fig. 5. DSC curves of precursor for $Zr(SO_4)_2/\gamma\text{-}Al_2O_3$ having different $Zr(SO_4)_2$ contents.

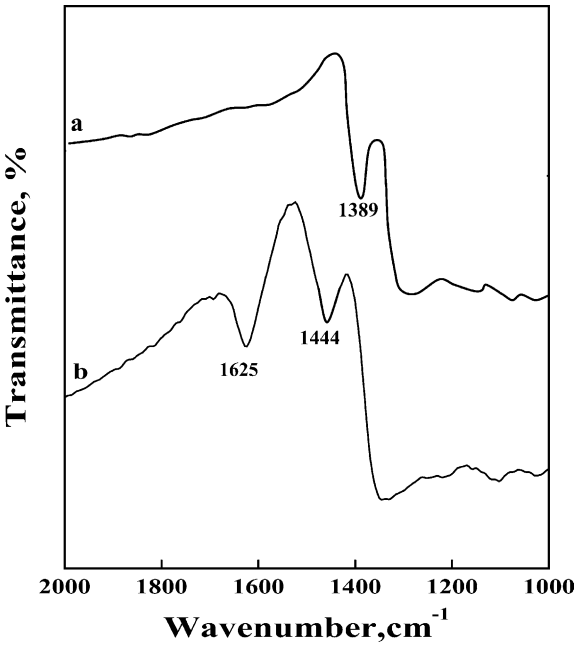


Fig. 6. Infrared spectra of $NH_3$ adsorbed on 20-$Zr(SO_4)_2/\gamma\text{-}Al_2O_3$: (a) background of 20-$Zr(SO_4)_2/\gamma\text{-}Al_2O_3$ evacuated at 400 °C for 1 h; (b) ammonia (2.67 kPa) adsorbed on (a); gas phase was evacuated at 230 °C for 1 h after adsorption in (b).

specific surface area, acid strength, and nature of acid centers (Brönsted or Lewis type). The specific surface areas of samples calcined at 400 °C for 2 h are listed in Table 1. The surface area showed a gradual decrease with increasing $Zr(SO_4)_2$ content.

The acidity of catalysts calcined at 400 °C, as determined by the amount of $NH_3$ irreversibly adsorbed at 230 °C [14–16], is listed in Table 1. The acidity increases with increasing zirconium sulfate content up to 40 wt.% of $Zr(SO_4)_2$.

Table 1
Specific surface area and acidity of $Zr(SO_4)_2/\gamma\text{-}Al_2O_3$ calcined at 400 °C for 2 h

| Catalysts | Specific surface area ($m^2$/g) | Acidity (μmol/g) |
|---|---|---|
| $\gamma\text{-}Al_2O_3$ | 240.0 | 155.0 |
| 10-$Zr(SO_4)_2/\gamma\text{-}Al_2O_3$ | 230.6 | 206.4 |
| 20-$Zr(SO_4)_2/\gamma\text{-}Al_2O_3$ | 206.8 | 244.9 |
| 30-$Zr(SO_4)_2/\gamma\text{-}Al_2O_3$ | 150.7 | 342.8 |
| 40-$Zr(SO_4)_2/\gamma\text{-}Al_2O_3$ | 131.7 | 418.7 |
| 50-$Zr(SO_4)_2/\gamma\text{-}Al_2O_3$ | 42.5 | 184.8 |
| 60-$Zr(SO_4)_2/\gamma\text{-}Al_2O_3$ | 23.8 | 85.6 |

Infrared spectroscopic studies of ammonia adsorbed on solid surfaces have made it possible to distinguish between Brönsted and Lewis acid sites [22,24,25]. Fig. 6 shows the IR spectra of ammonia adsorbed on 40-$Zr(SO_4)_2/\gamma\text{-}Al_2O_3$ samples evacuated at 400 °C for 1 h. For 40-$Zr(SO_4)_2/\gamma\text{-}Al_2O_3$, the band at 1444 $cm^{-1}$ is the characteristic peak of ammonium ion, which is formed on the Brönsted acid sites and the absorption peak at 1625 $cm^{-1}$ is contributed by ammonia coordinately bonded to Lewis acid sites [22,24,25], indicating the presence of both Brönsted and Lewis acid sites on the surface of 40-$Zr(SO_4)_2/\gamma\text{-}Al_2O_3$ sample. Other samples having different zirconium sulfate content also showed the presence of both Lewis and Brönsted acids. The intense band at 1389 $cm^{-1}$ after evacuation at 400 °C is assigned to the asymmetric stretching vibration of S=O bonds having a high double-bond nature [20,26]. However, the drastic shift of the IR band from 1389 $cm^{-1}$ to lower wavenumber (not shown due to the overlaps of skeletal vibration bands of $\gamma\text{-}Al_2O_3$) after ammonia adsorption (Fig. 6(b)) indicates a strong interaction between an

adsorbed ammonia molecule and the surface complex. Namely, the surface sulfur compound in the highly acidic catalysts has a strong tendency to reduce the bond order of SO from a highly covalent double-bond character to a lesser double-bond character when a basic ammonia molecule is adsorbed on the catalysts [20–22].

Acid stronger than $H_0 \leq -11.93$, which corresponds to the acid strength of 100% $H_2SO_4$, are superacids [1–3,27]. The strong ability of the sulfur complex to accommodate electrons from a basic molecule such as ammonia is a driving force to generate superacidic properties [20,26]. The 1390–1370 bands representing the asymmetric stretching of S=O is often regarded as the characteristic band of sulfated superacids [21,28]. As shown in Fig. 2, the asymmetric stretching bands of S=O after evacuation at 100–500 °C appeared at 1380–1394 $cm^{-1}$ differently depending on the evacuation temperature. The acid strength of $Zr(SO_4)_2/\gamma\text{-}Al_2O_3$ samples after evacuation at 500 °C for 1 h was also examined by a color change method, using Hammet indicator [29,30] in sulfuryl chloride. The samples were estimated to have $H_0 \leq -14.5$, indicating the formation of superacidic sites. Consequently, $Zr(SO_4)_2/\gamma\text{-}Al_2O_3$ catalysts would be solid superacids, in analogy with the case of $ZrO_2$ modified with sulfate group [14,16,17].

### 3.5. Catalytic activities for acid catalysis

It is interesting to examine how the catalytic activity of acid catalyst depends on the acid property. The catalytic activities for the 2-propanol dehydration are measured and the results are illustrated as a function of $Zr(SO_4)_2$ content in Fig. 7, where reaction temperatures are 160–180 °C. In view of Table 1 and Fig. 7, the variations in catalytic activity for 2-propanol dehydration are well correlated with the changes of their acidity, showing the highest activity and acidity for 40-$Zr(SO_4)_2/\gamma\text{-}Al_2O_3$. It has been known that 2-propanol dehydration takes place very readily on weak acid sites [31,32]. Good correlations have been found in many cases between the acidity and the catalytic activities of solid acids. For example the rates of both the catalytic decomposition of cumene and the polymerization of propylene over $SiO_2$–$Al_2O_3$ catalysts were found to increase with increasing acid

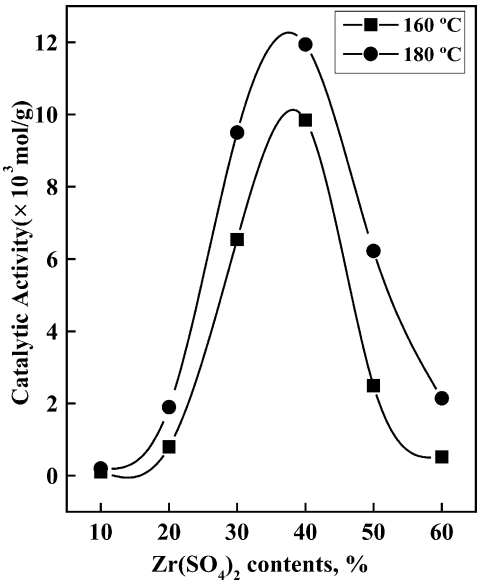


Fig. 7. Catalytic activities of $Zr(SO_4)_2/\gamma\text{-}Al_2O_3$ for 2-propanol dehydration as a function of $Zr(SO_4)_2$ content.

amounts at strength $H_0 \leq +3.3$ [33]. It was also reported that the catalytic activity of nickel silicates in the ethylene dimerization as well as in the butene isomerization was closely correlated with the acidity of the catalyst [34].

Cumene dealkylation takes place on relatively strong acid sites of the catalysts [31,32]. Catalytic activities for cumene dealkylation against $Zr(SO_4)_2$ content are presented in Fig. 8, where reaction temperature is 400–450 °C. Comparing Table 1 and Fig. 8, the catalytic activities are also correlated with the acidity. The correlation between catalytic activity and acidity holds for both reactions, cumene dealkylation and 2-propanol dehydration, although the acid strength required to catalyze acid reaction is different depending on the type of reactions. As seen in Figs. 7 and 8, the catalytic activity for cumene dealkylation, in spite of higher reaction temperature, is lower than that for 2-propanol dehydration.

Catalytic activities of 40-$Zr(SO_4)_2/\gamma\text{-}Al_2O_3$ for 2-propanol dehydration are plotted as a function of calcination temperature in Fig. 9. The activities increased with the calcination temperature, giving a maximum at 400 °C and then the activities decreased. Catalytic activities of 40-$Zr(SO_4)_2/\gamma\text{-}Al_2O_3$ for cumene dealkylation are also plotted as a function

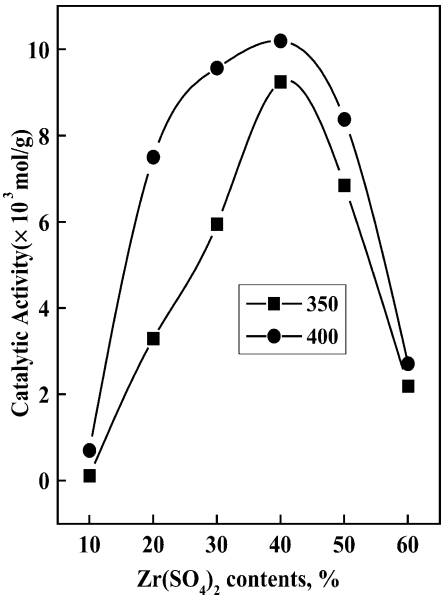


Fig. 8. Catalytic activities of $Zr(SO_4)_2/\gamma\text{-}Al_2O_3$ for cumene dealkylation as a function of $Zr(SO_4)_2$ content.

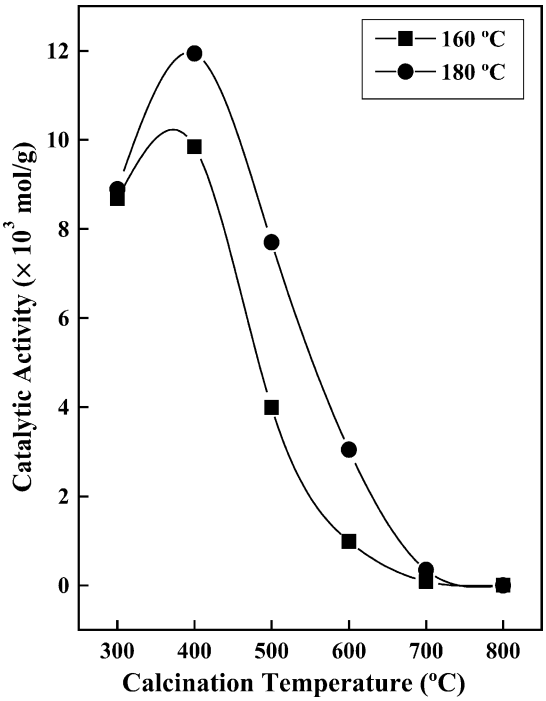


Fig. 9. Catalytic activities of 40-$Zr(SO_4)_2/\gamma\text{-}Al_2O_3$ for 2-propanol dehydration as a function of calcination temperature.

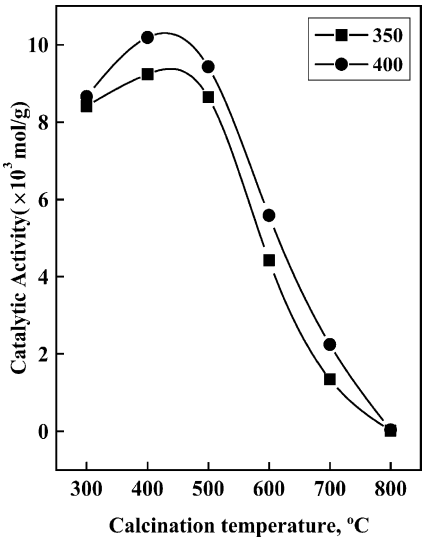


Fig. 10. Catalytic activities of 40-$Zr(SO_4)_2/\gamma\text{-}Al_2O_3$ for cumene dealkylation as a function of calcination temperature.

of calcination temperature in Fig. 10. The activities also exhibited a maximum at 400 °C. The decrease of activity for both reactions above 400 °C can be attributed to the fact that the surface area and acidity above 400 °C decrease with the calcination temperature.

## 4. Conclusions

This paper has shown that a combination of FTIR, DSC, and XRD can be used to perform the characterization of $Zr(SO_4)_2/\gamma\text{-}Al_2O_3$ prepared by impregnation of powdered $Zr(OH)_4$ with zirconium sulfate aqueous solution followed by calcining in air. The interaction between zirconium sulfate and $\gamma\text{-}Al_2O_3$ influenced the physicochemical properties of prepared catalysts with calcination temperature. The acidity of catalysts increase in proportion to the zirconium sulfate content up to 40 wt.% of $Zr(SO_4)_2$. The acid strength of $Zr(SO_4)_2/\gamma\text{-}Al_2O_3$ samples was estimated to have $H_0 \leq -14.5$, indicating the formation of superacidic sites. The correlation between catalytic activity and acidity holds for both reactions, cumene dealkylation and 2-propanol dehydration, although the acid strength required to catalyze acid reaction is different depending on the type of reactions.

## Acknowledgements

This work was supported by grant no. R05-2003-000-10074-0 from the Basic Research Program of the Korea Science and Engineering Foundation.

## References

[1] T.K. Cheung, J.L. d'Itri, F.C. Lange, B.C. Gates, Catal. Lett. 31 (1995) 153.
[2] K. Tanabe, M. Misono, Y. Ono, H. Hattori, New Solid Acids and Bases, Elsevier, Amsterdam, 1989, p. 215.
[3] K. Arata, Adv. Catal. 37 (1990) 165.
[4] D.A. Ward, E.I. Ko, J. Catal. 150 (1994) 18.
[5] S.R. Vaudagna, R.A. Comelli, S.A. Canavese, N.S. Figoli, J. Catal. 169 (1997) 389.
[6] L.M. Kustov, V.B. Kazansky, F. Figueras, D. Tichit, J. Catal. 150 (1994) 143.
[7] A. Sayari, Y. Yang, X. Song, J. Catal. 167 (1997) 346.
[8] C.Y. Hsu, C.R. Heimbuch, C.T. Armes, B.C. Gates, J. Chem. Soc., Chem. Commun. (1992) 1645.
[9] T.K. Cheung, B.C. Gates, J. Catal. 168 (1997) 522.
[10] T. Hosoi, T. Shimadzu, S. Ito, S. Baba, H. Takaoka, T. Imai, N. Yokoyama, Prepr. Symp. Div. Petr. Chem., American Chemical Society, Los Angeles, 1988, p. 562.
[11] K. Ebitani, J. Konishi, H. Hattori, J. Catal. 130 (1991) 257.
[12] M. Signoretto, F. Pinna, G. Strukul, P. Chies, G. Cerrato, S.D. Ciero, C. Morterra, J. Catal. 167 (1997) 522.
[13] K. Arata, M. Hino, N. Yamagata, Bull. Chem. Soc. Jpn. 63 (1990) 244.
[14] J.R. Sohn, E.H. Park, J. Ind. Eng. Chem. 4 (1998) 197.
[15] J.R. Sohn, S.G. Cho, Y.I. Pae, S. Hayashi, J. Catal. 159 (1996) 170.
[16] J.R. Sohn, M.Y. Park, J. Ind. Eng. Chem. 4 (1998) 84.
[17] J.R. Sohn, H.W. Kim, M.Y. Park, E.H. Park, J.T. Kim, S.E. Park, Appl. Catal. A: Gen. 128 (1995) 127.
[18] O. Saur, M. Bensitel, A.B.H. Saad, J.C. Lavalley, C.P. Tripp, B.A. Morrow, J. Catal. 99 (1986) 104.
[19] B.A. Morrow, R.A. McFarlane, M. Lion, J.C. Lavalley, J. Catal. 107 (1987) 232.
[20] C. Miao, W. Hua, J. Chen, Z. Gao, Catal. Lett. 37 (1996) 187.
[21] T. Jin, T. Yamaguchi, K. Tananbe, J. Phys. Chem. 90 (1986) 4794.
[22] J.R. Sohn, W.C. Park, Appl. Catal. A: Gen. 239 (2003) 269.
[23] W. Hua, Y. Xia, Y. Yue, Z. Gao, J. Catal. 196 (2000) 104.
[24] J.R. Sohn, T.D. Kwon, S.B. Kim, J. Ind. Eng. Chem. 7 (2001) 441.
[25] A. Satsuma, A. Hattori, K. Mizutani, A. Furuta, A. Miyamoto, T. Hattori, Y. Murakami, J. Phys. Chem. 92 (1988) 6052.
[26] J.R. Sohn, E.H. Park, H.W. Kim, J. Ind. Eng. Chem. 5 (1999) 253.
[27] F.G.A. Olah, G.K.S. Prakash, J. Sommer, Science 206 (1979) 13.
[28] C. Miao, W. Hua, J. Chen, Z. Gao, Catal. Lett. 37 (1996) 187.
[29] J.R. Sohn, S.G. Ryu, Langmuir 9 (1993) 126.
[30] J.R. Sohn, S.Y. Lee, Appl. Catal. A: Gen. 164 (1997) 127.
[31] J.R. Sohn, H.J. Jang, J. Mol. Catal. 64 (1991) 349.
[32] S.J. Decanio, J.R. Sohn, P.O. Paul, J.H. Lunsford, J. Catal. 101 (1986) 132.
[33] K. Tanabe, Solid Acids and Bases, Kodansha, Tokyo, 1970, p. 103.
[34] J.R. Sohn, A. Ozaki, J. Catal. 61 (1980) 29.